Line shape of electroreflectance spectra in semiconductor superlattices

U. Behn
Fachhochschule Schmalkalden, Blechhammer 4 und 9, D-98564 Schmalkalden, Germany

H. T. Grahn and K. Ploog
Paul-Drude-Institut für Festkörperelektronik, Hausvogteiplatz 5–7, D-10117 Berlin, Germany

H. Schneider
Fraunhofer-Institut für Angewandte Festkörperphysik, Tullastrasse 78, D-79108 Freiburg, Germany
(Received 22 June 1993)

Electroreflectance (ER) spectra of GaAs-AlAs superlattices in a perpendicular electric field exhibit complicated line shapes that cannot be explained by the presence of heavy-hole and light-hole excitonic transitions alone. Calculations of the absorption and ER spectra have been performed to investigate the influence of interference effects and transitions between continuum states on the corresponding line shape. Interference effects can lead to additional structures in the ER spectra that can be misinterpreted as additional transitions. A comparison of the experimental and calculated spectra shows that the presence of continuum states can contribute to the ER spectra. In this case, experimental ER spectra can only be simulated if contributions from band-to-band transitions and interference effects are taken into account. Therefore, a total of four rather than just the two excitonic transitions (heavy and light hole) are used.

I. INTRODUCTION

In the past decade it has been shown that modulation spectroscopy is a powerful tool for the investigation of semiconductor quantum-well (QW) and superlattice (SL) structures. In particular, electroreflectance (ER) and photoreflectance (PR), which, to some extent, is a modification of electroreflectance without using contacts, are ideal methods for studying the optical properties of quantum wells and superlattices in an electric field applied perpendicular to the layers. The observed effects include the quantum-confined Stark effect,[1,2] Wannier-Stark localization,[3–5] and the interaction of Wannier-Stark ladders originating from different subbands.[6–9] The advantages of ER and PR spectroscopy over other optical methods, such as transmission (absorption), photoluminescence, and photocurrent (PC) spectroscopy, are based on their differential character resulting in very sharp spectra without any background even at room temperature. Due to the complicated line shape, however, the interpretation of ER spectra is not as straightforward as in the other optical techniques mentioned. Usually it is necessary to fit the ER spectra to obtain the corresponding transition energies, whereas for the other techniques the peak positions, which can be determined very easily, yield the transition energies directly. Nevertheless, ER spectra can often give much more information about the subband structure of QW's and SL's.

For the fitting procedure it is necessary to know the line shape of the corresponding transitions, which contribute to the ER spectra. In the past most spectra have been computed using a Gaussian or a Lorentzian absorption profile.[10–12] In many spectra, however, neither of the two absorption profiles alone leads to a satisfactory fit and additional transitions have to be included. These additional transitions can originate from monolayer fluctuations[9,13] or the upper miniband edge.[14] Numerical calculations for multiple-QW structures have shown that interference effects due to multiple reflections from the different quantum wells can modify the ER line shape very strongly.[15] We expect that interference can also play an important role in ER spectra of SL structures embedded between cladding layers. In this case, multiple reflections from the interfaces between the cladding layers and the SL can modify the line shape of the ER spectra.

We have investigated the resonant coupling of different electronic subbands over several periods in a GaAs-AlAs superlattice with ER spectroscopy.[9] For the resonance field strengths the coupling of the subbands leads to an anticrossing with an energy separation in the meV range. To fit these spectra a complete knowledge of the line shape of the participating transitions is necessary. However, even for field strengths away from the resonance condition we found that the fitting of the ER spectra is rather complicated. We will confine our discussion to the band-gap transitions originating from the first heavy hole ($H11$) and light hole ($L11$) to the lowest electronic subband. The Gaussian absorption profile can only provide a good fit in this region if, instead of the two excitonic transitions $H11$ and $L11$, four transitions are taken into account, while the Lorentzian absorption profile always results in poorer agreement. The question about the origin of these two additional transitions has led us to investigate the influence of interference effects and of the contribution of band-to-band transitions on the line shape of the ER spectra. While interference effects under certain circumstances can lead to additional spectral structures, the spectra of our sample are not significantly

0163-1829/93/48(16)/11827(6)/$06.00 ©1993 The American Physical Society

altered by this. However, the band-to-band transitions cannot be neglected and result in additional transitions which are observed in the ER spectra as well as in the PC spectra.

This paper is organized as follows. In Sec. II we will describe the sample and the experimental technique. Section III summarizes the principles of electroreflectance. In Sec. IV the measured ER and PC spectra are presented and discussed. Section V is devoted to the calculation of the line shapes of the ER spectra for several layer configurations. The calculated line shapes are compared with the experimental results. A brief summary is given in Sec. VI.

II. EXPERIMENTAL

The 60-period GaAs-AlAs SL was grown by molecular beam epitaxy on a n^+ substrate with a well width of $d_{\mathrm{GaAs}} = 7.0$ nm and a barrier width of $d_{\mathrm{AlAs}} = 0.9$ nm. The superlattice was embedded in a p^+-i-n^+ diode with contact layers consisting of $Al_{0.5}Ga_{0.5}As$. On both sides of the superlattice a wide GaAs quantum well was sandwiched between the SL and the contact layers. A simplified schematic diagram including the widths of the layers of the full structure is shown in Fig. 1. The sample was structured into mesas of 450 μm diameter and supplied with Ohmic Cr/Au contacts on the top and AuGe/Ni contacts on the substrate side. The built-in voltage was about 1.5 V.

Electroreflectance and photocurrent spectroscopy measurements were performed in a flow cryostat at 77 K in a standard configuration at normal incidence. For the ER spectra the change in the reflectivity was directly normalized to the reflectivity at the same wavelength. We used a modulation amplitude of 0.2 V at a frequency of 360 Hz.

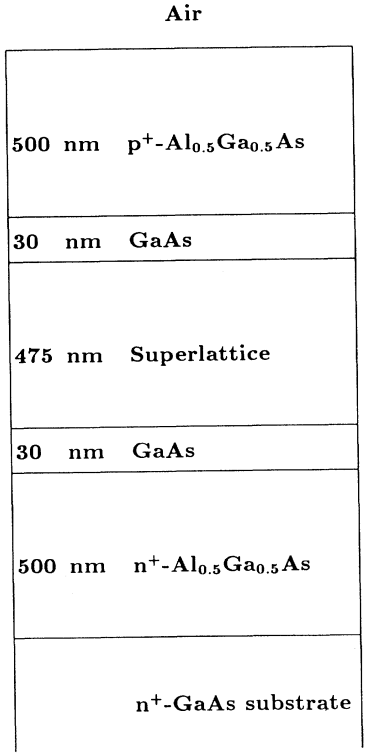

FIG. 1. Schematic diagram of the p-i-n structure.

III. PRINCIPLES OF ELECTROREFLECTANCE

The ER signal $\Delta R/R$ can be related to the complex dielectric function $\epsilon = \epsilon_1 + i\epsilon_2$ using the Seraphin coefficients[16]

$$\frac{\Delta R}{R} = \alpha\,\Delta\epsilon_1 + \beta\,\Delta\epsilon_2\,, \tag{1}$$

where $\Delta\epsilon_1$ and $\Delta\epsilon_2$ are the real and imaginary parts of the change of the dielectric function ϵ and $\Delta R/R$ is the change of the reflectivity due to the electric field modulation. The Seraphin coefficients α and β depend on the optical constants and the geometrical structure of the sample. For quantum wells and superlattices the field dependence of the change in the dielectric function can be written as[11,17]

$$\Delta\epsilon = \left[\frac{\partial\epsilon}{\partial E_g}\frac{\partial E_g}{\partial F} + \frac{\partial\epsilon}{\partial\Gamma}\frac{\partial\Gamma}{\partial F} + \frac{\partial\epsilon}{\partial I}\frac{\partial I}{\partial F}\right]\Delta F\,, \tag{2}$$

where E_g is the transition energy (e.g., of the exciton or band gap), Γ and I are the corresponding linewidth and oscillator strength, respectively, and F is the electric field strength. Usually the first term in Eq. (2) dominates. Therefore, we will restrict the discussion to the modulation of the dielectric function through the change in the band gap. An excitonic absorption profile L_2 is typically assumed to have a Gaussian

$$L_2(E,E_g,\Gamma) = \frac{1}{\sqrt{2\pi}\,\Gamma}\,\exp\left(-\frac{(E-E_g)^2}{2\Gamma^2}\right) \tag{3}$$

or Lorentzian

$$L_2(E,E_g,\Gamma) = \frac{\Gamma/\pi}{(E-E_g)^2+\Gamma^2} \tag{4}$$

line shape. E denotes the photon energy. The profile of the real part of the dielectric function L_1 can be calculated from the absorption profile via the Kramers-Kronig transform. The line shape of the electroreflectance signal is then determined according to Eq. (2) by the derivative of the real and imaginary parts of the dielectric function with respect to the gap energy E_g. Figure 2 shows the line shapes of ϵ_1 and ϵ_2 for Gaussian and Lorentzian absorption profiles and their derivatives. The main difference between the two line shapes lies in the fact that the Lorentzian has much larger wings. At the same time the linewidth, i.e., the full width at half maximum, is smaller by a factor of 0.85 for a Lorentzian than for a Gaussian. Looking at the line shape of $\partial\epsilon_1/\partial E_g$ one can distinguish between Gaussian and Lorentzian line shapes by defining the ratio of the amplitude of the minimum A to the amplitude of the side lobes B. For a Gaussian absorption profile the ratio A/B has a value of 3.5, while for a Lorentzian it is considerably larger ($A/B = 7.8$). The measured ER signal is usually a superposition of the

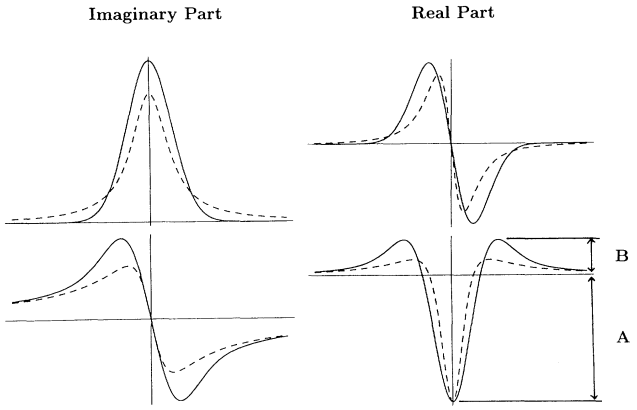

FIG. 2. Line shape of the real and imaginary parts of the dielectric function (upper curves) and its derivative with respect to the transition energy (lower curves) for a Gaussian (solid line) and Lorentzian (dashed line) absorption profile. The ratio A/B has a value of 3.5 for a Gaussian and 7.8 for a Lorentzian.

two line shapes shown in the lower part of Fig. 2. It can be directly proportional to either $\Delta\epsilon_1$ or $\Delta\epsilon_2$ depending on the Seraphin coefficients of the investigated sample, which can be estimated from the thickness of the overlayers and their respective optical constants.

The simulation of experimentally obtained ER spectra with the two line-shape profiles mentioned above is not always possible. In the case of symmetrical line shapes (see Fig. 2) the observed ratio A/B is sometimes even smaller for a Lorentzian than for a Gaussian. However, a superposition with additional weaker transitions originating from, e.g., monolayer fluctuations, band-to-band transitions, or upper miniband edge transitions can also lead to a change in this ratio. At the same time it should also affect the symmetry of the line shape, which also varies through the contribution from the change in the real and imaginary parts of the dielectric function. This leads us to the main point of this paper: the inclusion of band-to-band transitions and interference effects due to the layered structure. Before describing the calculation of the line shapes of the ER spectra from first principles, we want to defend the inclusion of these effects by presenting the experimental data in the next section.

IV. EXPERIMENTAL ELECTROREFLECTANCE AND PHOTOCURRENT SPECTRA

A series of ER spectra as a function of the applied voltage has been measured on the sample described in Sec. II. The sample shows the formation of Wannier-Stark ladders and resonant coupling between Stark ladders originating from different subbands as discussed in Ref. 6. We will restrict the discussion to field regions, where the Wannier-Stark localization is complete but no resonant coupling is present. In order to perform a line-shape analysis in the region of resonant coupling, it is important to first understand the ER spectra in the field regions, where no splitting of transitions occurs. In Fig. 3 an ER and a PC spectrum at -4 V (corresponding to

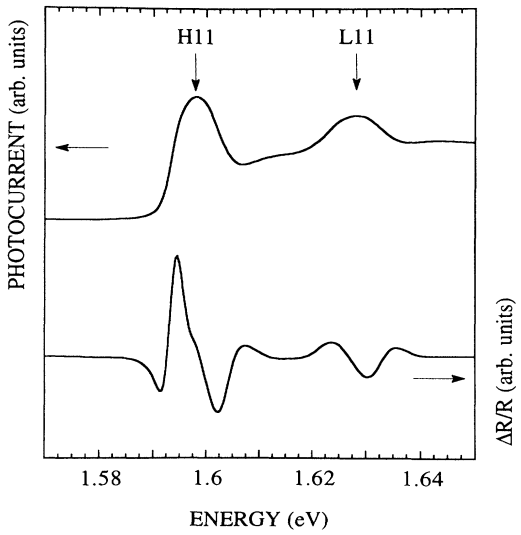

FIG. 3. Measured photocurrent and electroreflectance spectra of the superlattice for an applied voltage of -4 V at 77 K.

an electric field strength of approximately 103 kV cm^{-1}) is displayed. The PC spectrum clearly shows the excitonic resonances at 1.598 eV of the $H11$ and at 1.628 of the $L11$ transition. Furthermore, approximately 13 meV above the $H11$ and $L11$ transitions a small shoulder is observed, which is most likely due to transitions between the band edges of the continuum states. The separation is considerably larger than one would expect from monolayer fluctuations with an estimated energy separation of about 8–9 meV. In the lower part of the figure the ER spectrum measured at the same applied voltage exhibits line shapes that cannot be fitted satisfactorily using either a Gaussian or a Lorentzian absorption profile if only the two excitonic transitions ($H11$ and $L11$) are assumed. The ratio A/B defined in Fig. 2 has a value of 2.2 (B is taken to be the mean value of both side lobes in this case), which is considerably smaller than for the Gaussian line profile. In addition, in the $H11$ line at 1.598 eV a shoulder is observed, which coincides with the energy value of the PC maximum for this transition. The $H11$ and $L11$ transitions in the ER spectrum have nearly opposite phases. A decent fit of the line shape of the ER spectrum in Fig. 3 can only be achieved if four transitions with a Gaussian profile are used instead of two. The resulting transition energies are listed in Table I. This rather phenomenological approach of analyzing the ER spectra is not very satisfying. In the next section, we will present a

TABLE I. Energies of the $H11$ and $L11$ transitions obtained from a fit with a total of four Gaussian oscillators of the experimental ER spectrum at -4 V.

$H11$	1.594 eV
	1.602 eV
$L11$	1.622 eV
	1.631 eV

model taking into account the layered structure and the band-to-band transitions to determine the line shape in a straightforward manner.

V. NUMERICAL SIMULATION OF THE LINE SHAPE

We perform a straightforward calculation of the line shape of the ER spectra. First, we estimate the dielectric function of the superlattice and all the cladding layers. The corresponding complex index of refraction is given by $n(E,F) = \sqrt{\epsilon(E,F)}$. With the knowledge of the index of refraction and the layer thickness of each layer, the reflectance, the imaginary part of the dielectric function or absorption, and transmission of different sample configurations is evaluated using the recurrent method,[18,19] which provides the same results as a transfer matrix method.[20] To compute the ER signal $\Delta R/R$ the reflectance has to be evaluated at two different field strengths. Taking the difference $\Delta R = R(E, F_{\rm dc} + F_{\rm ac}) - R(E, F_{\rm dc})$, where $F_{\rm dc}$ and $F_{\rm ac}$ are the unmodulated and modulated parts of the applied electric field, and dividing it by the mean value of both reflectances leads to the desired quantity $\Delta R/R$.

The line shape of the resulting ER spectrum is dominated by the characteristics of the superlattice, since only the intrinsic region of the sample (cf. Fig. 1) is influenced by the electric field modulation. To estimate the superlattice dielectric function we use a semi-empirical approach following Klipstein and Aspley,[10] modeling the continuum by taking the band-to-band contribution as a group of Lorentzian oscillators with a constant density of states D_{2D} beginning at the band-gap energy E_g. The corresponding phenomenological dielectric function can be written in the following form:

$$\epsilon(E) = 13.25 + \sum_{H11,L11} \left[C^{\rm ex}\, L^{\rm ex}(E, E_{\rm ex}, \Gamma^{\rm ex}) + D_{2D}\, C^{\rm bb} \int_{E_g}^{\infty} L^{\rm bb}(E, E', \Gamma^{\rm bb})\, dE' \right] , \tag{5}$$

where $L^{\rm ex} = L_1^{\rm ex} + iL_2^{\rm ex}$ and $L^{\rm bb}$ denote the complex line shape of excitonic and band-to-band transitions, respectively, and $C^{\rm ex}$ and $C^{\rm bb}$ the corresponding amplitude factors. In our calculations the excitonic absorption profile $C^{\rm ex}L_2^{\rm ex}$ is assumed to be Gaussian. To calculate the ER spectra we assume that the modulation of the electric field only influences the position of the transition energies, neglecting changes in the linewidth and intensity [cf. Eq. (2)]. This implies that the main contribution to the change of the dielectric function due to the electric field modulation originates from the quantum-confined Stark effect [the first term in Eq. (2)] for both the excitonic and the band-to-band transitions. Therefore, we expect an ER line shape, which corresponds to the first derivative of the dielectric function and not to the third derivative, as in the case of band-to-band transitions in bulk semiconductors in the low-field limit of the Franz-Keldysh theory.[21]

First, we will investigate the influence of the band-to-band transitions onto the PC and ER spectra. In this case we will use a simple geometrical model for the whole SL structure, which considers the SL as a semi-infinite effective medium with one transparent $Al_{0.5}Ga_{0.5}As$ overlayer. Since the PC spectrum mainly reflects the absorption of the SL, we show in Fig. 4 the calculated spectral dependence of ϵ_2 in the energy region of the $H11$ and $L11$ transitions. The transition energies are taken from the experiment and the ratio of the heavy-hole to light-hole oscillator strength is assumed to be 3.5. The inclusion of band-to-band transitions not only gives the background signal above the $L11$ excitonic transition, but also reproduces the observed shoulders above the $H11$ and $L11$ transitions. The ratio of the amplitudes of excitonic and band-to-band transitions is taken from the experimental PC spectrum in Fig. 3. For a better comparison of the ER spectra computed with purely excitonic effects and the inclusion of band-to-band transitions we have adjusted the overlayer thickness of the simulated structure to achieve a symmetrical line shape for the purely excitonic case. This implies that the change in the reflectance is proportional to $\Delta\epsilon_1$, i.e., β in Eq. (1) is zero. To discuss the influence of the band-to-band transitions it is sufficient to consider only the $H11$ transition. In Fig. 5 the dashed line represents a calculated ER spectrum, which only takes into account the excitonic transition with a ratio A/B of 3.0. The solid line in Fig. 5 denotes the ER spectrum, where excitonic as well as band-to-band transitions are included. The ratio A/B is lowered to 2.2 and an additional positive wing appears on the high energy side. The ratio of excitonic and band-to-band contributions is the same as in the absorption spectrum in Fig. 4. It is evident from Fig. 5 that the inclusion of band-to-band transitions significantly alters the ER line shape and therefore cannot be neglected for this particular structure. The ratio A/B is in good agreement with

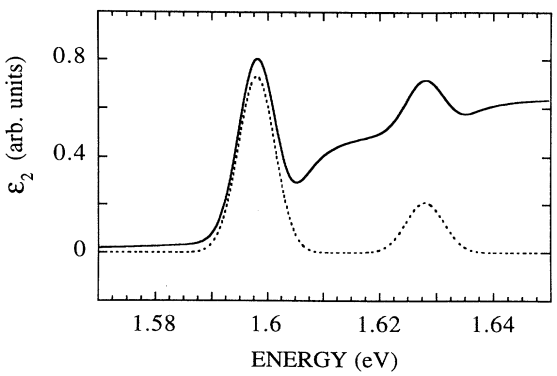

FIG. 4. Calculated spectrum of the imaginary part of the dielectric function. The dashed line denotes ϵ_2 taking only excitonic transitions into account. The solid line shows the result when band-to-band transitions are included.

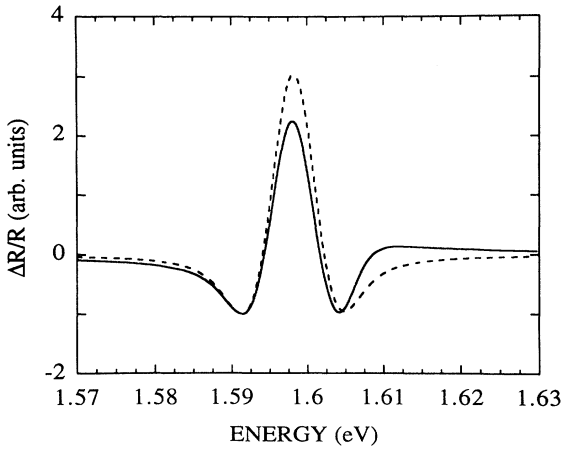

FIG. 5. Calculated electroreflectance spectrum of the $H11$ transition assuming a semi-infinite superlattice with only one overlayer. The dashed line denotes $\Delta R/R$ taking only the excitonic part into account. The solid line shows the result when the band-to-band part is also included.

the experimental observation (Fig. 3).

To discuss the influence of interference effects on the ER spectra we first neglect, for simplicity, the band-to-band transitions. Interferences are included by calculating the reflectance of the complete superlattice structure as shown in Fig. 1. The dielectric functions of the different GaAs and $Al_xGa_{1-x}As$ cladding layers are assumed to be constant in the narrow spectral region under consideration. The absorption in the $Al_xGa_{1-x}As$ layers is neglected. In Fig. 6, two calculated ER spectra are displayed which differ only by the total thickness

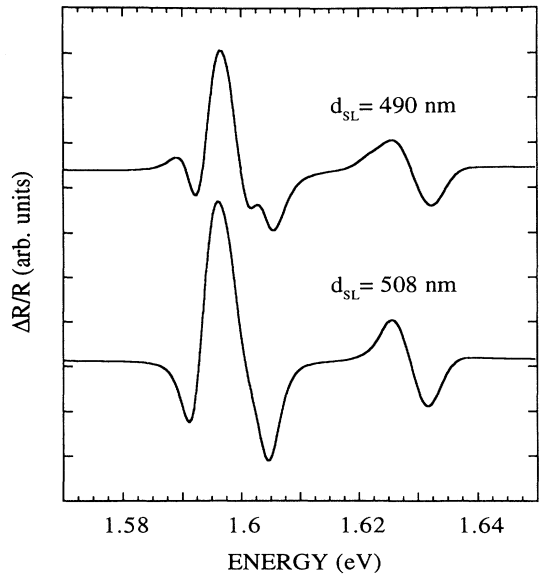

FIG. 6. Calculated electroreflectance spectra of the complete superlattice structure shown in Fig. 1 neglecting band-to-band transitions. In this case both transitions, i.e., $H11$ and $L11$, are shown. The upper curve corresponds to a total SL thickness of 490 nm, while the lower one refers to a SL thickness of 508 nm.

of the superlattice. The interference effects that appear by varying the layer thickness can drastically alter the line shape, which can be mistaken for the appearance of additional transitions. In particular, the $H11$ transition is strongly affected due to the lower absorption in the superlattice in this energy range. A similiar result was obtained by Shields and Klipstein,[15] taking into account the multiple reflections of the individual well-barrier interfaces of a QW structure.

To simulate the experimentally obtained ER and PC spectra we now include band-to-band transitions in the calculation. The exciton binding energy of the $H11$ and $L11$ transitions is assumed to be 8 meV, in agreement with the fitted ER data (Table I), whereas the used broadening parameter of 3.5 meV is estimated from the experimental PC spectrum (half width at half maximum). The thicknesses of the superlattice region (508 nm) and the top contact layer (500 nm) were adjusted within experimental uncertainty to achieve a decent agreement of the calculated spectrum with the experimental spectrum. Figure 7 shows the resulting ER and absorption spectra, which are in very good agreement with the experimental curves without using a fitting procedure. The phase relation between the $H11$ and $L11$ transitions turns out to be nearly the same as in the experiment. The experimentally observed shoulder in the ER spectrum (Fig. 3), which is also seen in the lower curve of Fig. 6, where only excitonic transitions are included, could only be simulated by taking lower values of the broadening parameter. This, in turn, leads to a poorer agreement between the experimentally detected and simulated PC spectra. The absorption spectrum is not very different from the bare absorption spectrum of the SL shown in Fig. 4. The effect of interference on the line shape is much more pronounced in the ER spectrum

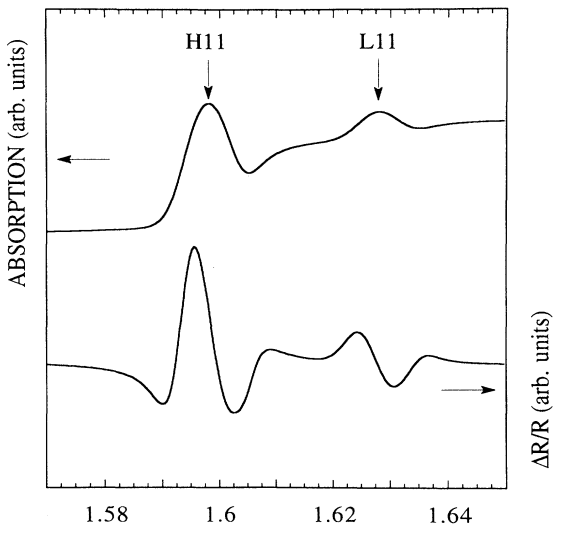

FIG. 7. Calculated absorption and electroreflectance spectra of the complete layer structure including band-to-band transitions and interference effects for a SL thickness of 508 nm.

than in the absorption spectrum. This is to be expected, since electroreflectance, due to its derivative character, is much more sensitive to small changes in the effective dielectric function than absorption spectroscopy. We have not attempted to fit the experimental ER spectrum to our model, since the agreement is already very good. At the same time the number of adjustable parameters is too large.

VI. SUMMARY

The line shape of electroreflectance spectra of a GaAs-AlAs superlattice has been measured and compared to simulations. In addition to the usual excitonic transitions, our model for the line-shape calculation takes into account contributions from band-to-band transitions and interference effects originating from multiple reflections in the superlattice due to the cladding layers. Satisfactory agreement between the measured and calculated line shapes is achieved only when both effects are included. These results are relevant for all ER spectra (and also PR spectra) with several transitions energetically close together.

ACKNOWLEDGMENTS

We would like to thank G. Gobsch and N. Stein at the Technische Universität in Ilmenau for use of their laboratory equipment and technical support. This work was supported in part by the Bundesminister für Forschung und Technologie.

[1]D.A.B. Miller, D.S. Chemla, T.C. Damen, A.C. Gossard, W. Wiegmann, T.H. Wood, and C.A. Burrus, Phys. Rev. Lett. **53**, 2173 (1984).
[2]A.J. Shields, P.C. Klipstein, J.S. Roberts, and C. Button, Superlatt. Microstruct. **7**, 409 (1990).
[3]E.E. Mendez, F. Agulló-Rueda, and J.M. Hong, Phys. Rev. Lett. **60**, 2426 (1988).
[4]P. Voisin, J. Bleuse, C. Bouche, S. Gaillard, C. Alibert, and A. Regreny, Phys. Rev. Lett. **61**, 1639 (1988).
[5]M. Nakayama, I. Tanaka, T. Doguchi, H. Nishimura, K. Kawashima, and K. Fujiwara, Solid State Commun. **77**, 303 (1991).
[6]H. Schneider, H.T. Grahn, K. von Klitzing, and K. Ploog, Phys. Rev. Lett. **65**, 2720 (1990).
[7]M. Nakayama, I. Tanaka, H. Nishimura, K. Kawashima, and K. Fujiwara, Phys. Rev. B **44**, 5935 (1991).
[8]I. Tanaka, M. Nakayama, H. Nishimura, K. Kawashima, and K. Fujiwara, Phys. Rev. B **46**, 7656 (1992).
[9]U. Behn, H.T. Grahn, H. Schneider, and K. Ploog, in *Quantum Well and Superlattice Physics IV*, edited by G.H. Döhler and E.S. Koteles (SPIE, Bellingham, 1992), p. 298.
[10]P.C. Klipstein and N. Aspley, J. Phys. C **19**, 6461 (1986).
[11]B.V. Shanabrook, O.J. Glembocki, and W.T. Beard, Phys. Rev. B **35**, 2540 (1987).
[12]O.J. Glembocki and B.V. Shanabrook, Superlatt. Microstruct. **3**, 235 (1987).
[13]A.J. Shields, P.C. Klipstein, J.S. Roberts, and C. Button, Phys. Rev. B **42**, 3599 (1990).
[14]H. Shen, S.H. Pan, F.H. Pollak, M. Dutta, and T.R. AuCoin, Phys. Rev. B **36**, 9384 (1987).
[15]A.J. Shields and P.C. Klipstein, Phys. Rev. B **43**, 9118 (1991).
[16]B.O. Seraphin and N. Bottka, Phys. Rev. **145**, 628 (1966).
[17]O.J. Glembocki and B.V. Shanabrook, Superlatt. Microstruct. **5**, 603 (1989).
[18]U. Behn and H. Röppischer, J. Phys. C **21**, 5507 (1988).
[19]P.H. Berning, in *Physics of Thin Films,* edited by G. Hass (Academic, New York, 1963), Vol. 1, p.69.
[20]M. Born and E. Wolf, *Principles of Optics*, 6th ed. (Pergamon, Oxford, 1980), p. 55.
[21]D.E. Aspnes, Surf. Sci. **37**, 418 (1973).